# Appendix C: Food Webs



#### 1 Introduction

The production and transfer of energy within an ecosystem (ecosystem energetics) is a key functional process, fundamental to determining population and community structure and system productivity. The production and transfer of energy in an ecosystem begins with nutrient and light availability driving primary production, in turn creating basal resources that are transferred along a myriad of pathways to higher order consumers. Water for the environment influences *Water Quality* (nutrients, temperature, light, and salinity), which in turn can regulate rates of *Metabolism* and productivity (carbon and energy availability) and this energy fuels the trophic carrying capacity of *Food webs* (microinvertebrates and macroinvertebrates) that support fish and waterbird populations. This chapter integrates these fundamental ecosystem processes, linking environmental watering actions to water quality, energy production and understanding the potential food web responses within key habitats of the Junction of the Warrego and Darling rivers Selected Area (Warrego-Darling Selected Area, Selected Area).

Specifically, this chapter links the Water Quality, Metabolism, Microinvertebrate and Macroinvertebrate indicators into one integrated chapter. Answering the questions, what did Commonwealth environmental water contribute to:

- Temperature regimes?
- pH levels?
- Turbidity regimes?
- Salinity regimes?
- Dissolved oxygen levels?
- Algal suppression?
- Patterns and rates of primary productivity?
- Patterns and rates of decomposition?
- Microinvertebrate and macroinvertebrate productivity?
- Microinvertebrate and macroinvertebrate diversity?
- Microinvertebrate and macroinvertebrate community composition?
- Connectivity of microinvertebrate and macroinvertebrate communities in floodplain watercourses?

## 1.1 Previous monitoring

Five years of LTIM water quality, metabolism and microinvertebrate and macroinvertebrate monitoring has highlighted that increased flows in the Warrego-Darling Selected Area consistently improved water quality parameters such as electrical conductivity, pH and salinity through dilution due to higher water volume. During connection, the Warrego River water improved the water quality in the Darling River downstream of the confluence. In the Warrego channel and Western Floodplain, concentrations of nitrogen and phosphorus were consistently higher than Australian and New Zealand Environment and Conservation Council (ANZECC) and Queensland Department of Environment and Science guideline values and concentrations were found to increase as water levels contracted (time since connection or inundation). Levels of primary production followed patterns of nutrient availability and temperature, with maximum productivity in summer low flow conditions. There was evidence from

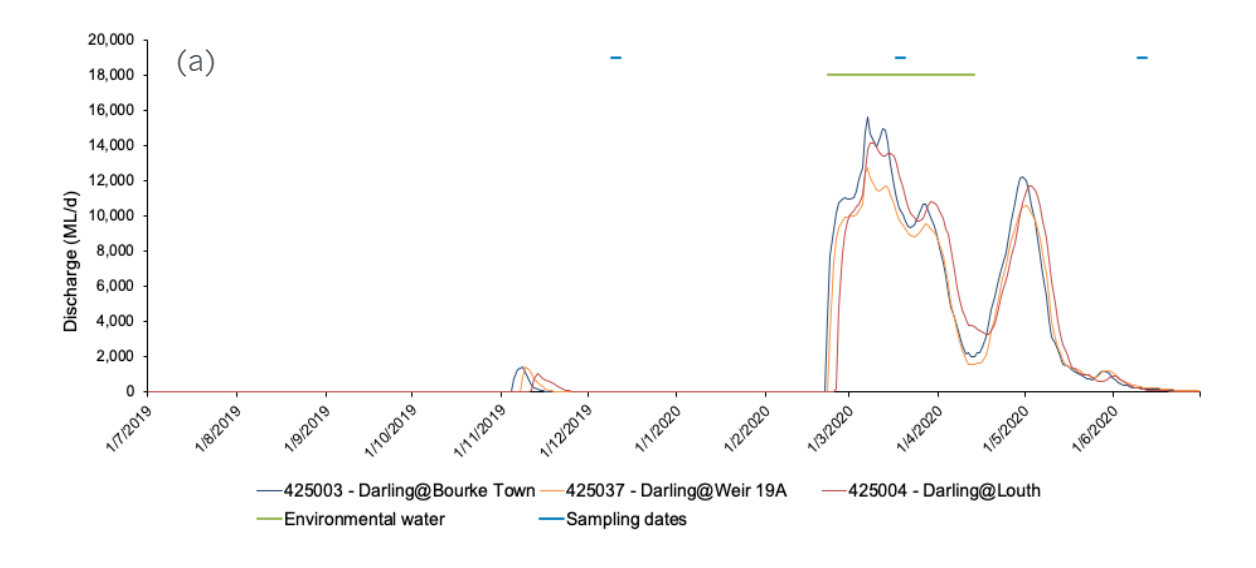
ad hoc sampling of thermal stratification in the deeper pools of the Darling River, but the stratification was not sufficient to produce any harmful ecological impacts. Stream metabolism rates were highly variable and consistently heterotrophic (consuming more carbon than producing) and increased with increasing in-stream Total Nitrogen and chlorophyll a concentrations, suggesting primary productivity rates were predominantly driven by nutrient availability and temperature. Increased discharge and associated increased turbidity are the key limitations to rates of productivity.

Microinvertebrates and macroinvertebrates were the only ecological indicators monitored in all Warrego channel, Western Floodplain and Darling River sites. Similar trends were observed for both indicators: invertebrate communities of the Western Floodplain displaying higher density, richness and diversity when inundated; Warrego channel sites being intermediate; and the Darling River communities showing the lowest density, richness and diversity. For communities on the Western Floodplain and Warrego channel, flow elicited a positive response, stimulating primary production, improving water quality, and increasing access to habitat. When inundated, the Western Floodplain provided ideal slow-flow invertebrate habitat and, coupled with the increased nutrients and basal resources with wetting, drove booms in invertebrate productivity. Peaks of diversity and richness were observed 30-50 days after connection in the Warrego channel and 100 days on the floodplain, with populations then declining as water levels receded and water quality deteriorated. As time since connection increased, species with a higher tolerance to poor water quality dominated. The seasonal timing of flow events also appears to influence the magnitude of the invertebrate response through the regulation of metabolic rates by temperature. During the largest inundation event on the Western Floodplain in winter 2016, the boom in microinvertebrate biomass did not occur immediately after inundation, instead the boom was delayed until warmer temperatures and increased rates of primary production were evident.

## 2 Methods

# 2.1 Field and laboratory methods

Three sampling events were undertaken in the 2019-20 water year: December 2019, March 2020 and June 2020. In relation to the flow and inundation that commenced February/March 2020, these sampling times acted as before, during and after the flow (Appendix A: Darling River Hydrology, Appendix B: Warrego River Hydrology, Figure 1). Loggers were deployed during the December 2019 sampling trip and downloaded in March and June 2020.



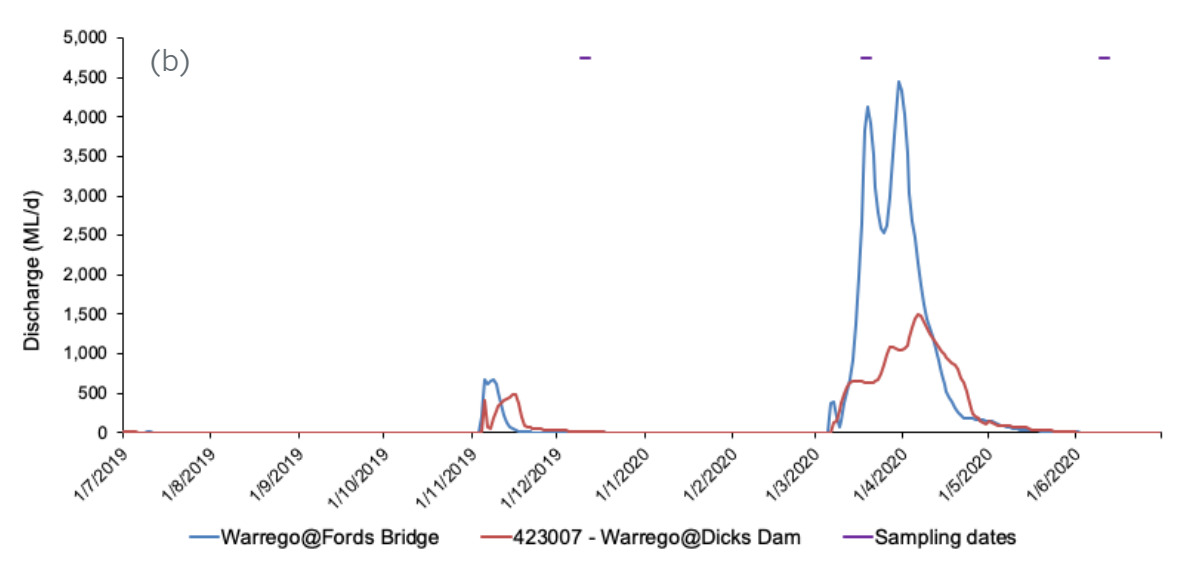


Figure 1 Hydrograph showing the duration of Flow Event 1 (green line) and sampling dates in (a) the Darling River and (b) the Warrego River.

Samples were taken from sites in the Darling River, 7 sites in the Warrego channel and 3 sites on the Western Floodplain (Table 1, Figure 2).

Table 1 Warrego-Darling Selected Area Foodweb sampling sites.

Zone	Site code	Latitude	Longitude
Darling River	AKUNA	-30.4098	145.334
Darling River	DARPUMP	-30.4046	145.446
Warrego River	BOERA1	-30.0994	145.428
Warrego River	BOERA2	-30.1	145.43
Warrego River	BOOKA1	-30.196	145.435
Warrego River	BOOKA2	-30.2	145.44
Warrego River	ROSS1	-30.3903	145.41
Warrego River	ROSS2	-30.39	145.41
Warrego River	DICKS	-30.3175	145.359
Western Floodplain	WF1	-30.1138	145.423
Western Floodplain	WF2	-30.1309	145.42
Western Floodplain	WF3	-30.1742	145.416

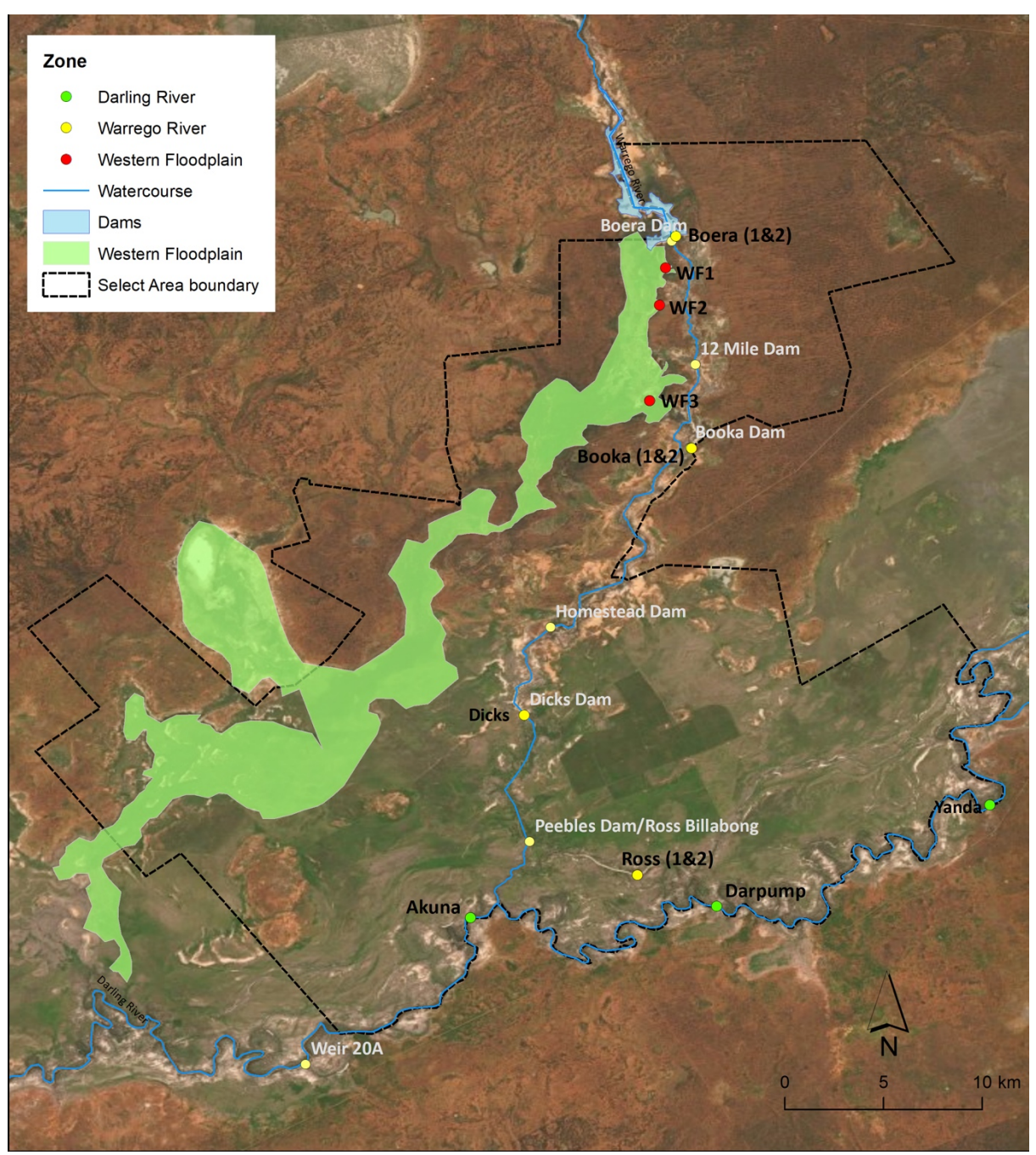


Figure 2 Map of sampling sites for water quality, stream metabolism and invertebrate parameters in the Darling River, Warrego River and Western Floodplain.

Stream metabolism measurements were performed according to the LTIM Standard Methods (Hale *et al.* 2014), updated to align with the BASEv2 model. Water temperature and dissolved oxygen (DO) were logged every ten minutes using PME MiniDOT loggers that optically measure DO. Two of the three study zones were measured in the 2019-20 water year. Two sites were measured in the Darling River Zone: the upstream site at the Darling Pumps and the downstream site near Akuna homestead (Figure 2). Three sites were measured in the Warrego River Zone: Boera Dam, Booka Dam and Ross Billabong (Figure 2). Metabolism was not measured in the Western Floodplain during 2019-20, although water quality, microinvertebrates and macroinvertebrates were sampled at all three sites once the floodplain was inundated (Figure 2). Light and

atmospheric pressure loggers were deployed at Toorale and also logged at 10-minute intervals.

Water quality variables were also measured as *in situ* spot recordings using a Hydrolab Quanta multi-probe (temperature (°C), electrical conductivity (mS/cm), dissolved oxygen (mg/L, % saturation), pH, and turbidity (NTU)) in December 2019, March 2020 and June 2020, following the LTIM Standard Methods (Hale *et al.* 2014). Water samples were taken for analysis of TN ( $\mu$ g/L), oxides of nitrogen (NOx,  $\mu$ g/L), Total Phosphorus (TP,  $\mu$ g/L), Filterable Reactive Phosphorus (FRP,  $\mu$ g/L), Chlorophyll *a* (Chla,  $\mu$ g/L) and dissolved organic carbon (DOC,  $\mu$ g/L).

Inorganic nutrients were sampled at 0.2 m depth at each site by filling 125 mL thrice-rinsed pre-labelled PET bottles with raw river water and freezing samples until analysis. Dissolved inorganic nutrients were filtered through rinsed Whatman GF/C filters (effective pore size 0.7  $\mu m$ ). TN and TP were prepared using a simultaneous persulphate digestion (Hosomi and Sudo 1986). TN, NOx, TP and FRP were determined colorimetrically: TN and NOx at 543 nm after cadmium-copper reduction (Wood  $et\ al.$  1967), and TP and FRP at 705 nm after using a molybdite-antimony procedure (Murphy and Riley 1962). All absorption spectra were measured using a UC-1700 Pharmaspec UV-visible spectrometer.

Chlorophyll a samples were collected by filtering as much water as possible (100-1000 mL) through a Whatman GF/C filter paper feffective pore size 0.7  $\mu$ m) using an electric vacuum pump (EYELA Tokyo Rakahikai Corporation Aspirator A-35 at approximately 7 PSI). Filter papers were placed into pre-labelled 10 mL vials that were wrapped in aluminium foil and refrigerated below 4 °C. Chlorophyll a was calculated colorimetrically by digesting the sample in 10 mL 90 % acetone at 4 °C for 24 hours, centrifuging the samples and reading the absorption spectra at 665 and 750 nm using a UV-1700 Pharmaspec UV-visible spectrometer.

DOC samples were pre-filtered using Whatman glass microfiber GF/C filters (effective pore size 0.7  $\mu$ m), then through Whatman cellulose acetate filters (0.2  $\mu$ m pore size), then frozen until analysis. Samples were analysed using the supercritical water oxidation technique (GE Analytical Instruments) using an InnovOx Total Organic Carbon Analyser (GE Analytical Instruments).

Microinvertebrates were sampled in December 2019, March 2020 and June 2020. Samples taken in June will be reported in the 2020-21 report. Samples were collected from benthic and pelagic habitats, preserved and identified according to the LTIM Standard Methods (Hale *et al.* 2014). Benthic microinvertebrates were sampled by compositing five cores (50 mm diameter with 250 mL volume) for each site, leaving to settle for 15 minutes and decanting through a 63  $\mu$ m sieve. The retained samples were preserved in ethanol (70 % w/v with Rose Bengal stain). Pelagic microinvertebrates were sampled from 90 L of water column at each site, retained in a 63  $\mu$ m plankton net and preserved in ethanol (70 % w/v with Rose Bengal stain) until identification. Microinvertebrates in homogenised subsamples were identified under a stereo microscope at 400x magnification. Identification was to family (rotifers and cladocerans), class (copepods) and ostracods. Subsample totals were scaled up to the total sample volume and reported as density/L.

Aquatic macroinvertebrates were also sampled in December 2019, March 2020 and June 2020, preserved and identified according to the LTIM Standard Methods (Hale *et al.* 2014). Samples taken in June will be reported in the 2020-21 report.

## 2.2 Data analysis

Water quality and nutrient data (spot measurements) were used to interpret patterns in stream metabolism and invertebrate community composition. DO, conductivity, pH, turbidity, chlorophyll a, TN, TP, NOx and FRP were analysed by log (x+1) transforming parameters where appropriate to ensure normality and homogeneity of variances, and analysing two-way ANOVAs with Time (with 3 fixed levels, December 2019, March 2020 and June 2020), Zone (with 3 fixed levels, Darling, Warrego and Western Floodplain) and the Time\*Zone interaction.

The acceptance criteria for the BASE model (Grace *et al.* 2015) to include daily results in further data analyses are that the fitted model for a day must have an  $r^2$  value  $\geq 0.90$ , coefficients of variation for the gross primary productivity (GPP), ecosystem respiration (ER) and K < 50%, and reaeration coefficients within the range of 0.1 to 0.9. The BASEv2 model also requires that the model fit parameter (PPfit) must be within the range 0.1 to 0.9. Acceptable daily values of GPP, ER and net primary production (NPP) were grouped into months and analysed by two-way ANOVAs with the factors of Time (fixed with 6 levels) and Site (fixed with 5 levels). Significant pairwise interactions were examined further using *post hoc* Tukey HSD tests.

Metabolic production and consumption of carbon can be extrapolated from GPP, ER and NPP rates, by multiplying each daily rate by daily discharge (>0 ML/day) and a molecular conversion factor (12/32) to exchange carbon for oxygen. There were limited days for the Darling River and Boera Dam where acceptable metabolic data coincided with discharge >0 ML/day, so one-way ANOVAs with Site (with 5 fixed levels) were used to analyse the 2019-20 dataset. Significant pairwise interactions were examined further using *post hoc* Tukey HSD tests.

Richness, density (individuals/L) and Shannon diversity were calculated separately for microinvertebrate and macroinvertebrates using the DIVERSE function in PRIMER V7 with PERMANOV+ V1.0.3 package (PRIMER-E 2009); pelagic and benthic microinvertebrate habitats were combined to calculate total microinvertebrate richness, density and diversity. Invertebrate richness for the 2019-20 water year was analysed in R using a two-way analysis of deviance as observations followed a Poisson distribution. The two factors were Time (with 2 fixed levels, Pre and During Event 1) and Zone (with 3 fixed levels, Darling, Warrego and Western Floodplain). Density and diversity followed quasipoisson distributions so were analysed using two-way analyses of variance with the same two factors of Time and Zone. Post hoc Tukey HSD tests were used to determine significant differences among the three Zones where relevant.

Multi-year analyses of microinvertebrate and macroinvertebrate richness followed the same procedure of analyses of deviance for richness and analyses of variance for density and diversity. The main effects for multi-year analyses were Time (with 4 fixed levels, 2015-16, 2016-17, 2017-18 and 2019-20) and Zone (with 3 fixed levels, Darling, Warrego and Western Floodplain). Post hoc Tukey HSD tests were used to determine significant differences among the four Times, three Zones and their interactions where relevant.

Community composition of invertebrates (microinvertebrates and macroinvertebrates combined) were analysed using multivariate techniques. PERMANOVA routine was used

to test the differences in richness, density and diversity, among Time (with 2 fixed levels, Pre and During flows), Zone (with 3 fixed levels, Darling, Warrego and Western Floodplain), and Site (with 6 fixed levels, AKUNA, DARPUMP, BOERA, BOOKA, ROSS and WF) where Site is nested within Zone. Up to 999 random permutations estimated the probability of p-values, with significance reported at p<0.05.

Bray-Curtis dissimilarity matrices were generated for density and presence-absence data to examine community composition among samples. Nonmetric multidimensional scaling ordinations (nMDS) were used to visualise differences among community compositions and SIMPER analyses were used to determine which taxa contributed to observed community patterns. nMDS outputs with stress <0.2 were considered appropriate for interpretation (Clarke and Warwick 2001).

Multiyear analyses were performed on the 2014-2020 dataset using PERMANOVA, where the factors were Time (sampling events with 12 random levels), Zone (with 3 fixed levels, Darling, Warrego and Western Floodplain), and Site (with 6 fixed levels, AKUNA, DARPUMP, BOERA, BOOKA, ROSS and WF) where Site is nested within Zone. Up to 999 random permutations estimated the probability of p-values, with significance reported at p<0.05.

Vectors of productivity (GPP, ER, NPP) were overlain on a PCA ordination to determine how stream metabolism influenced invertebrate communities among sites.

## 3 Results

# 3.1 2019-20 water year

#### 3.1.1 Water chemistry

Spot measurements of DO only fell below the ANZECC (2000) guidelines in the Western Floodplain in March 2020, with readings of 2.80 mg/L at WF1 and 3.68 mg/L at WF2 (Table 2). DO ranged from a mean concentration of approximately 7.0 mg/L in March 2020 to approximately 11 mg/L in June 2020 (after significant flows and inundation) and was consistent across the Darling and Warrego Rivers within sampling times. There was high variability in DO levels among sites within zones and across times  $(F_{2,17}=18.952, p<0.001)$ . In contrast, the minimum DO in the Western Floodplain was  $3.24 \pm 0.62$  (SD) mg/L in March 2020 increasing to  $14.66 \pm 3.44$  mg/L in June 2020 following a peak in water column and benthic algal productivity. An algal bloom in June 2020 (chlorophyll a=223.82 µg/L) contributed to a very high daytime concentration of DO (17.19 mg O<sub>2</sub>/L) at WF1. Outside of this outlier, there were no significant differences in concentrations of chlorophyll a among sampling times, zones, or sites within zones, with mean concentrations ranging from  $8 \pm 4 \mu g/L$  in the Darling in March 2020 to 32 ± 31 µg/L in the Warrego River in June 2020 (Table 2). This was due to the high variability in chlorophyll a concentrations among sites, which became more homogeneous during flows and inundation.

Conductivity ranged from 0.09  $\pm$  0.01 mS/cm in the Warrego in March 2020 (during significant flows and inundation) to 0.12  $\pm$  0.01 in the Darling in June 2020 (post flows). Conductivity remained under ANZECC (2000) guidelines throughout the 2019-20 water year except for a minor exceedance of 0.312 mS/cm at WF1 in June 2020. There were

no significant patterns among Sites, Zones or Time. Increased pH was recorded in March 2020 across all Zones ( $F_{1,17}$ =95.939, p<0.001), although several significant pairwise Time\*Site (Zone) interactions confounded patterns among Zones or Sites ( $F_{2,15}$ =5.324, p=0.016). Nonetheless, all pH remained within ANZECC (2000) guidelines except for an alkaline value of 9.19 at WF1 in June 2020, again associated with the algal bloom and the localised production of carbonates.

Turbidity exceeded ANZECC (2000) guidelines in all sampling observations and by an order of magnitude of the guideline (50 NTU) in 60% of observations. Turbidity significantly decreased in the Darling (p<0.001) from a mean of 816  $\pm$  4.3 NTU in March 2020 to 216  $\pm$  6.4 NTU in June 2020. In contrast, ranges remained similar (433  $\pm$  82.3 – 531  $\pm$  107.2 NTU) in the Warrego and Western Floodplain (89  $\pm$  37 – 84  $\pm$  23 NTU) during flows and inundation.

There were no significant patterns in TN, TP or FRP between times, or among Zones and Sites (Zones). However, substantial exceedances of ANZECC (2000) guidelines were observed in all but two observations of TN and in all TP and FRP observations. Mean concentrations of TN ranged from 1099  $\pm$  328 to 2703  $\pm$  3740  $\mu g/L$  in the Warrego, 1129  $\pm$  65 to 1246  $\pm$  298  $\mu g/L$  in the Darling and 1860  $\pm$  2101 to 5174  $\pm$  1275  $\mu g/L$  in the Western Floodplain. Mean concentrations of TP ranged from 407  $\pm$  147 to 661  $\pm$  546  $\mu g/L$  in the Warrego, 377  $\pm$  28 to 530  $\pm$  64  $\mu g/L$  in the Darling and 419  $\pm$  447 to 668  $\pm$  306  $\mu g/L$  in the Western Floodplain. Mean concentrations of FRP ranged from 187  $\pm$  91 to 347  $\pm$  315  $\mu g/L$  in the Warrego, 135  $\pm$  11 to 146  $\pm$  33  $\mu g/L$  in the Darling and 79  $\pm$  34 to 484  $\pm$  125  $\mu g/L$  in the Western Floodplain (Table 2).

Nitrate-nitrate concentrations were greatest in the Darling (640  $\pm$  19 to 700  $\pm$  811  $\mu$ g/L), which was significantly greater than the Western Floodplain (26  $\pm$  35 to 181  $\pm$  19  $\mu$ g/L; p=0.004), but not the Warrego (256  $\pm$  78 to 327  $\pm$  281  $\mu$ g/L; F<sub>2,17</sub>=7.397, p<0.005). There was no significant temporal pattern, with concentrations increasing in the Darling and Warrego and decreasing in the Western Floodplain. With the exception of the Western Floodplain in June 2020, all NOx observations exceeded ANZECC (2000) guidelines (5  $\mu$ g/L) by more than an order of magnitude (Table 2).

Table 2 Spot measurements of water chemistry through the 2019-20 water year. \* indicates means of two readings are presented.

	DARPUMP	AKUNA	BOERA*	BOOKA*	DICKS	ROSS*	WF1	WF2
Temperature (°C)								
December 2019	24.4	26.0	27.1	24.8	26.5	25.9		
March 2020	23.7	24.7	25.7	27.3	27.9	24.0	23.1	24.5
June 2020	11.9	15.8	14.8	12.6	13.5	11.8	19.7	15.4
Conductivity (mS/cm)								
December 2019	0.144	0.270	0.132	0.142	0.078	0.222		
March 2020	0.148	0.142	0.110	0.096	0.069	0.089	0.142	0.085
June 2020	0.025	0.224	0.084	0.154	0.144	0.163	0.312	0.172
Salinity (PSS)								
December 2019	0.05	0.12	0.07	0.07	0.03	0.08		
March 2020	0.07	0.07	0.05	0.04	0.03	0.04	0.07	0.04
June 2020	0.12	0.11	0.07	0.07	0.07	0.08	0.15	0.08
Dissolved Oxygen (%)								
December 2019	88.2	89.8	82.3	85.4	98.4	87.0		
March 2020	85.8	83.0	80.0	93.2	109.4	78.1	32.8	44.1
June 2020	98.8	108.3	108.1	89.1	125.8	95.5	187.9	160.6
DO (mg/L)								
December 2019	7.26	7.35	7.16	7.81	7.88	7.09		
March 2020	7.27	6.90	6.47	7.39	8.59	6.46	2.80	3.68
June 2020	10.67	10.73	10.94	9.46	13.1	10.33	17.19	16.04
рН								
December 2019	7.71	7.52	7.13	7.05	7.31	7.21		
March 2020	7.58	7.43	7.10	7.18	7.29	7.28	6.99	6.80
June 2020	8.55	8.24	8.01	7.78	8.56	8.38	9.19	8.87
Turbidity (NTU)								
December 2019	517.9	493.8	411.7	416.2	395.7	323.4		

	DARPUMP	AKUNA	BOERA*	BOOKA*	DICKS	ROSS*	WF1	WF2
March 2020	818.7	812.6	453.9	521.8	429.0	324.6	63.1	115.1
June 2020	209.0	218.1	437.3	484.6	506.8	682.7	75.5	66.2
Chlorophyll a (mg/L)								
December 2019	10.370	14.127	12.722	20.114	36.771	37.102		
March 2020	5.540	10.654	7.144	30.393	32.074	33.204	54.292	10.552
June 2020	20.875	35.328	20.809	21.632	53.184	25.774	223.816	2.916
TN (µg/L)								
December 2019	1,090.4	972.1	806.2	698.4	423.2	2,075.7		
March 2020	1,175.7	1,083.2	829.0	744.2	405.2	7,685.7	6,075.5	4,272.7
June 2020	1,035.5	1,456.6	864.5	1,075.0	877.6	1,469.7	4,285.5	588.2
TP (µg/L)								
December 2019	290.9	309.1	349.1	346.2	291.5	514.1		
March 2020	575.5	485.2	458.6	354.4	142.3	539.7	884.6	452.0
June 2020	396.6	357.1	367.7	418.5	458.0	1,299.7	930.7	106.3
NOx (µg/L)								
December 2019	351.1	640.9	275.6	240.5	238.5	298.7		
March 2020	627.2	653.7	251.8	212.0	265.0	300.4	167.8	194.4
June 2020	126.7	1,273.0	149.3	458.5	172.0	451.0	66.4	6.0
FRP (µg/L)								
December 2019	120.6	110.0	134.2	127.9	196.6	372.4		
March 2020	169.3	122.1	133.6	136.8	131.1	319.3	572.1	395.2
June 2020	127.2	142.6	114.7	147.6	352.3	775.7	115.8	74.9

#### 3.1.2 Metabolism

Loggers were deployed in December 2019 and downloaded in March 2020 and June 2020. The acceptance rate for modelling each day's diel DO curve ranged from 7.6 % of all days logged at Boera Dam (12 days from 157 possible days), to 16.6 % at Ross Billabong (Table 3). One main reason for the low acceptance rates was due to poor model fit, with the correlation ( $R^2$ ) between the observed and modelled DO data of less than 0.80 for almost 80% of the modelling days. Median GPP ranged from 0.48 mg  $O_2/L/day$  at Ross Billabong (Table 4) to 8.88 mg  $O_2/L/day$  at the upstream site on the Darling River (DARPUMP, Table 5).

GPP decreased longitudinally downstream in both the Darling and Warrego Rivers (Figure 3,  $F_{4,75}$ =3.712, p<0.008), with GPP significantly greater in the upstream Darling site (DARPUMP) than the lower Warrego (i.e. BOOKA p<0.05 and ROSS p<0.05). ER was highest and most variable in the upstream Darling River (DARPUMP, Figure 3), and this was significantly greater ( $F_{4,75}$ =15.888, p<0.001) than in the lower Darling (i.e. AKUNA p<0.001) and the Warrego River (i.e. BOERA, BOOKA and ROSS p<0.001).

Despite the lower GPP at AKUNA not being statistically significant to DARPUMP, ER was significantly lower at AKUNA than DARPUMP (p < 0.001), which meant that NPP (Figure 3; F<sub>4,75</sub>=3.482, p<0.001) and P:R (Figure 3, F<sub>4,75</sub>=3.482, p<0.05) were significantly greater at AKUNA than DARPUMP (NPP p<0.001, P:R p<0.05, Table 3). NPP was also significantly lower in the Warrego River (Table 5) than DARPUMP (i.e. BOERA, BOOKA and ROSS p<0.001), although only ROSS had significantly higher P:R than DARPUMP (p<0.05). There were no clear temporal patterns in GPP, ER or NPP overall or within any site to indicate that February-May flows influenced productivity rates within the Warrego or Darling Rivers.

There were limited days for the Darling River and Boera Dam where acceptable metabolic data coincided with discharge > 0 ML/day, so one-way ANOVAs with Site (with 5 fixed levels) were used to analyse carbon dynamics in the 2019-20 dataset. Nonetheless, both the Darling and Warrego were strongly heterotrophic, i.e. more carbon was consumed by ecosystem respiration than was produced by photosynthesis (Figure 4). Carbon production at AKUNA ranged from 964 – 67,555 kg C/day (Figure 4), an order of magnitude greater than carbon production in the other sites  $(F_{4,26}=6.224, p<0.001)$ , particularly BOOKA (p<0.001) and ROSS (p<0.005) in the lower Warrego River, with its smaller discharge and lower rates of GPP. Likewise, consumption of carbon at AKUNA ranged from 3,380 – 323,512 kg C/day (Figure 4), which was significantly greater than in the lower Warrego ( $F_{4,26}$ =4.327, p<0.01), particularly BOOKA (p<0.01) and ROSS (p<0.01) which ranged 181 – 90,263 and 1,186 – 71,362 kg C/day, respectively. All sites were consistent carbon sinks, with net carbon consumption ranging from 2,416 – 255,957 kg C/day at AKUNA, significantly greater than the Warrego sites ( $F_{4.26}$ =5.950, p<0.005), due to both lower NPP and higher discharge. In particular, net carbon consumption ranged from 169 – 86,533 kg C/day at BOOKA (p<0.005) and 669 – 66,409 kg C/day at ROSS (p<0.005).

Carbon production and consumption through February-May 2020 flow event were totalled for each site for the days where both the BASE model assumptions were met and discharge > 0 ML/day. Commonwealth water for the environment constituted 12.2 % of February-May 2020 flow event (Event 1 in Appendix A: Darling River Hydrology) discharge, and carbon production and consumption were attributed to either CEW or non-CEW (Figure 5).

Table 3 Summary of logger deployments and data availability for the five logger sites in the Selected Area during January – June 2020.

Zone	Site	First Deployed	Last Deployed	Tota I Days	Days with Acceptabl e Data	% Acceptabl e Days
Darling	DARPUM P	03/01/202 0	09/06/202 0	157	18	11.5
River	AKUNA	03/01/202 0	09/06/202 0	157	15	9.6
	BOERA	03/01/202 0	09/06/202 0	157	12	7.6
Warreg o	BOOKA	03/01/202 0	09/06/202 0	157	22	14.0
	ROSS	03/01/202 0	09/06/202 0	157	26	16.6

Table 4 Summary of gross primary production (GPP, mg O2/L/day), ecosystem respiration (ER, mg O2/L/day), net primary production (NPP, mg O2/L/day) and P/R ratios for the three sites on the Warrego River from January – June 2020.

		В	OERA			BOO	OKA	
	Median	Mean	Min	Max	Median	Mean	Min	Max
GPP	4.97	5.22	0.40	14.00	3.77	4.49	0.87	11.38
ER	31.16	43.01	13.21	106.94	23.63	29.86	9.38	89.87
NPP	-27.36	-37.79	-105.91	-8.35	-17.15	-25.37	-86.15	-2.89
P/R	0.16	0.17	0.01	0.37	0.15	0.20	0.04	0.81
		R	OSS					
	Median	Mean	Min	Max				
GPP	8	5.41	1.43	14.01				
ER	24.16	30.11	5.87	76.84				
NPP	-19.94	-24.71	-71.51	0.27				
P/R	0.19	0.24	0.05	1.08				

Table 5 Summary of gross primary production (GPP, mg  $O_2/L/day$ ), ecosystem respiration (ER, mg  $O_2/L/day$ ), net primary production (NPP, mg  $O_2/L/day$ ) and P/R ratios for the two sites on the Darling River from January – June 2020.

	DARPUMP			AKUNA				
	Median	Mean	Min	Max	Median	Mean	Min	Max
GPP	8.88	9.78	0.08	28.00	5.57	6.09	0.27	14.01
ER	92.42	102.50	0.16	229.57	25.48	32.04	0.93	68.80
NPP	-81.81	-92.72	-0.08	-223.83	-20.06	-25.95	65.02	0.27
P/R	0.13	0.14	0.01	0.55	0.21	0.26	0.05	1.05

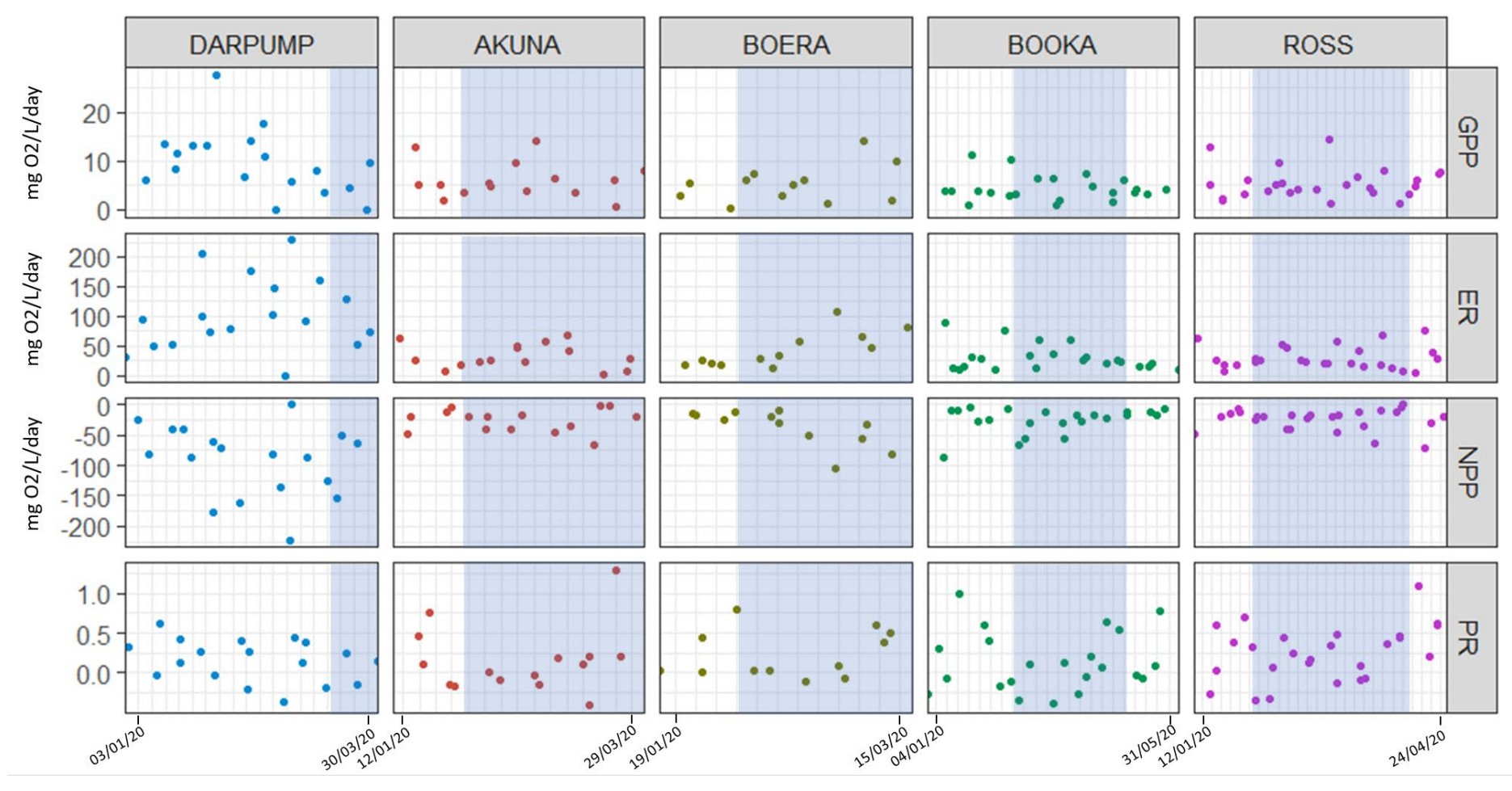


Figure 3 Gross primary productivity (GPP), ecosystem respiration (ER), net primary productivity (NPP) and P:R at sites in the Darling (DARPUMP and AKUNA) and Warrego Rivers (BOERA, BOOKA and ROSS). Blue time periods indicate the flow event.

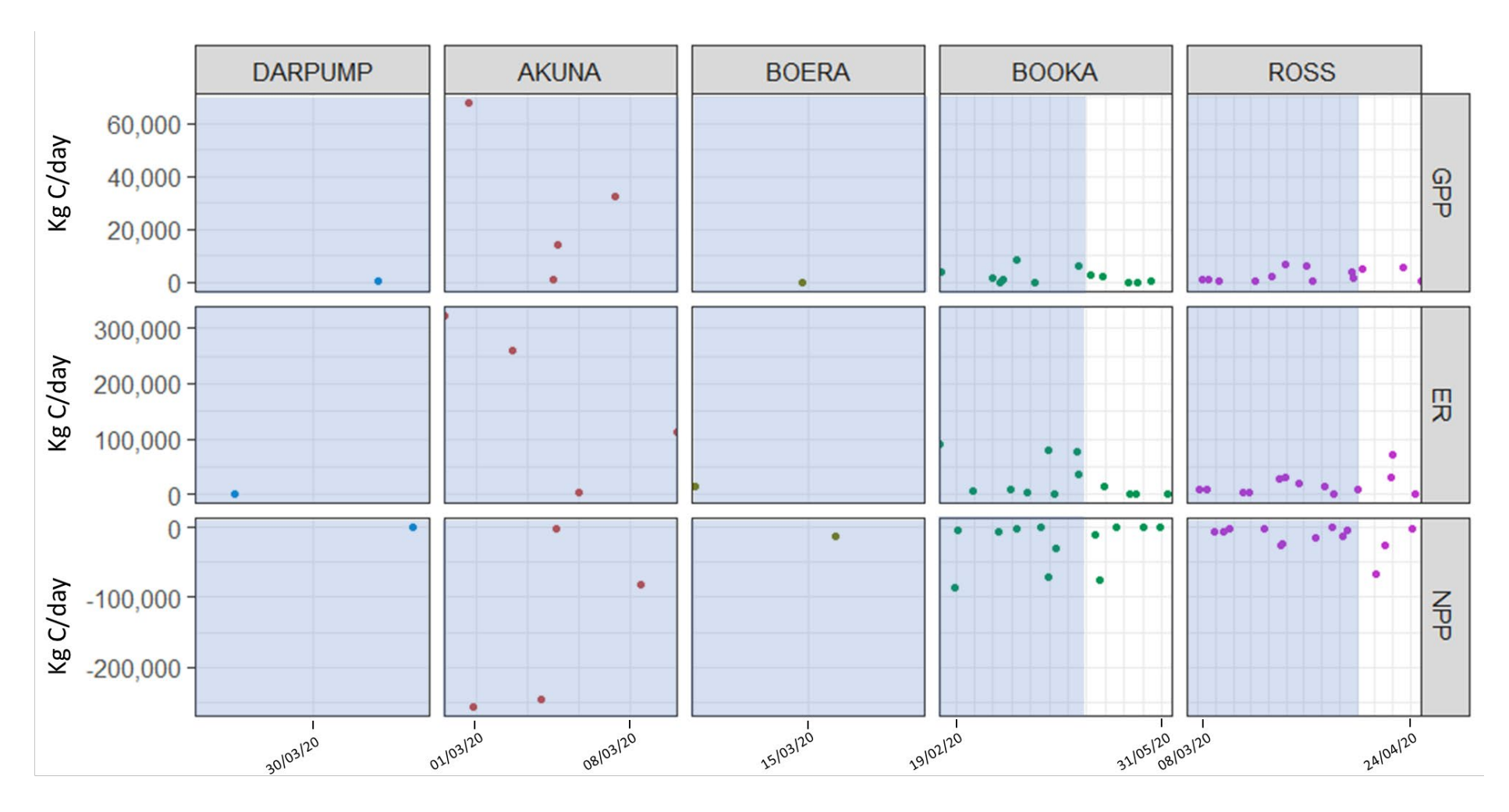


Figure 4 Carbon (kg/day) produced through GPP, consumed through ER and net result (NPP) in the Darling (DARPUMP and AKUNA) and Warrego Rivers (BOERA, BOOKA, ROSS). Blue time periods indicate the flow event. Data exist where BASE model outputs coexist for days where discharge was greater than 0 ML/day.

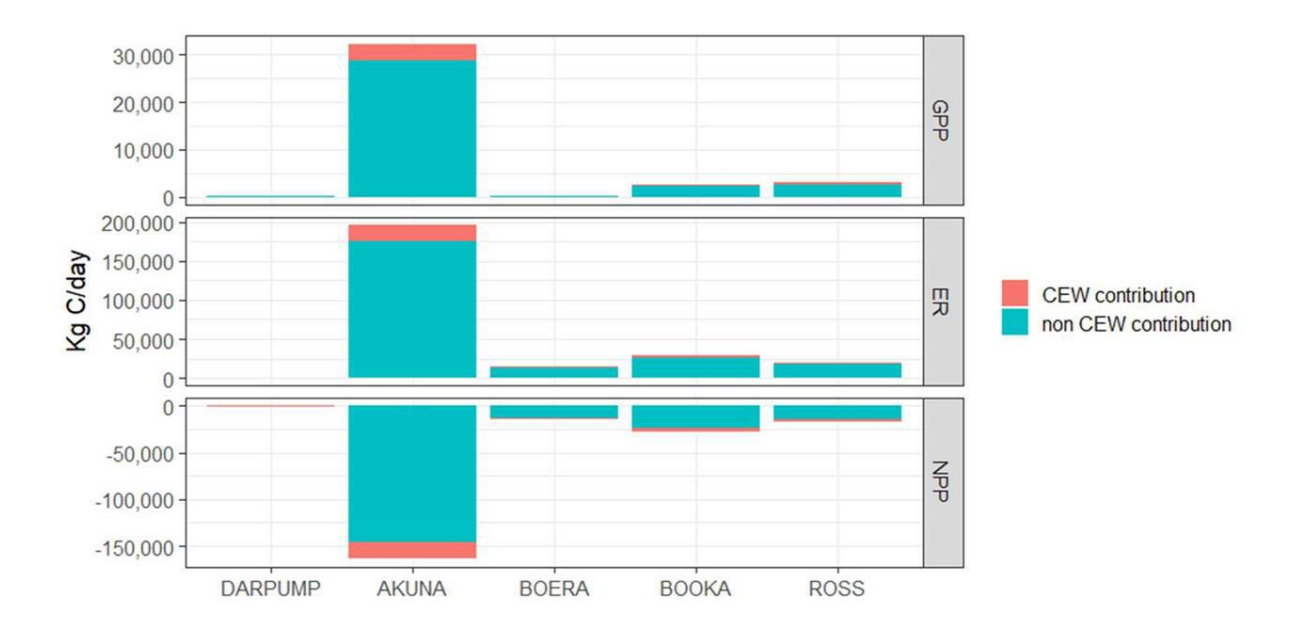


Figure 5 Proportion of carbon produced through GPP, consumed through ER and net result (NPP) in the Darling and Warrego Rivers. The upstream site on the Darling River (DARPUMP) had single data points in very low ranges that met model and discharge requirements. CEW indicates the proportion attributed to Commonwealth environmental water.

#### 3.1.3 Microinvertebrates

Microinvertebrate richness did not change from the December 2019 to March 2020 sampling (Figure 6). However, richness was significantly different among Zones (Figure 6,  $X^2_{2,15}$ =4.991, p<0.05), with higher richness in the Warrego (9.6 ± 0.9 taxa) than the highly variable responses in the Western Floodplain (6.5 ± 3.5, p<0.05), and most similar to the richness recorded in the Darling (9.0 ± 0.8). While the numbers of taxa comprising communities were similar pre and during flows, density fell significantly from pre flow conditions (1511 ± 614 individuals/L) to during flows (297 ± 118 individuals/L, Figure 7,  $X^2_{1,15}$ =65.624, p<0.001), across all Zones. Diversity remained similar across Time, Zones and Sites (Zones) (Figure 8).

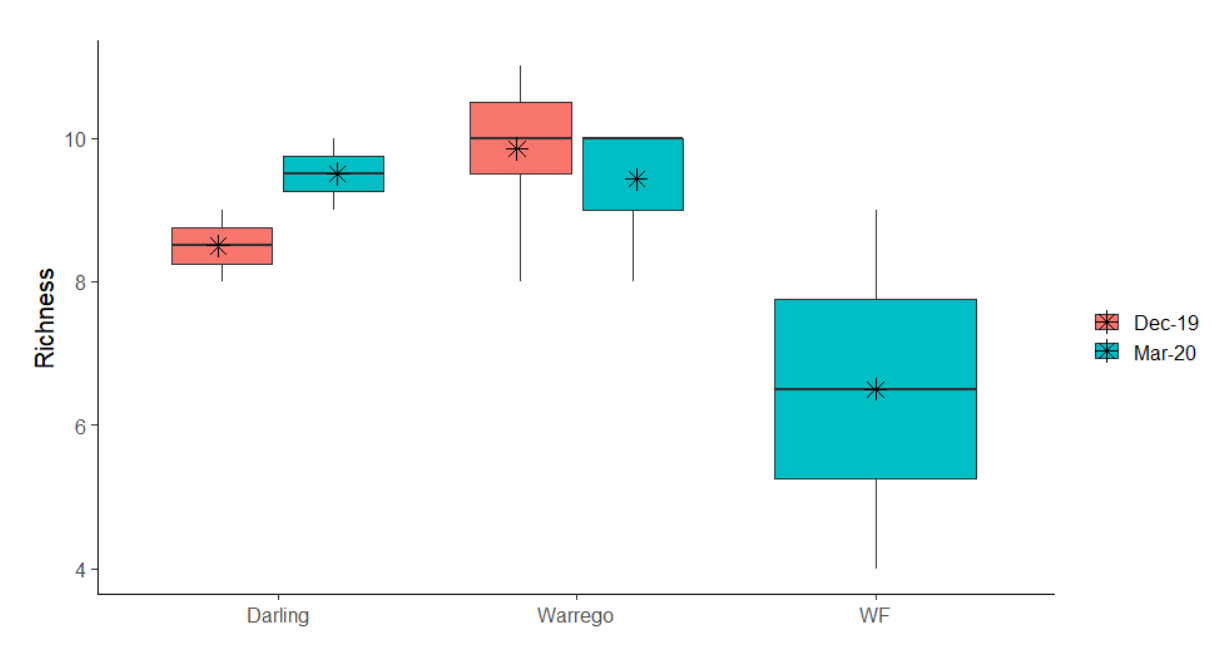


Figure 6 Ranges in microinvertebrate taxa richness Pre- (Dec 2019) and During (Mar 2020) flows in the 2019-2020 water year across the three Zones. Horizontal black lines indicate medians and asterisks means.

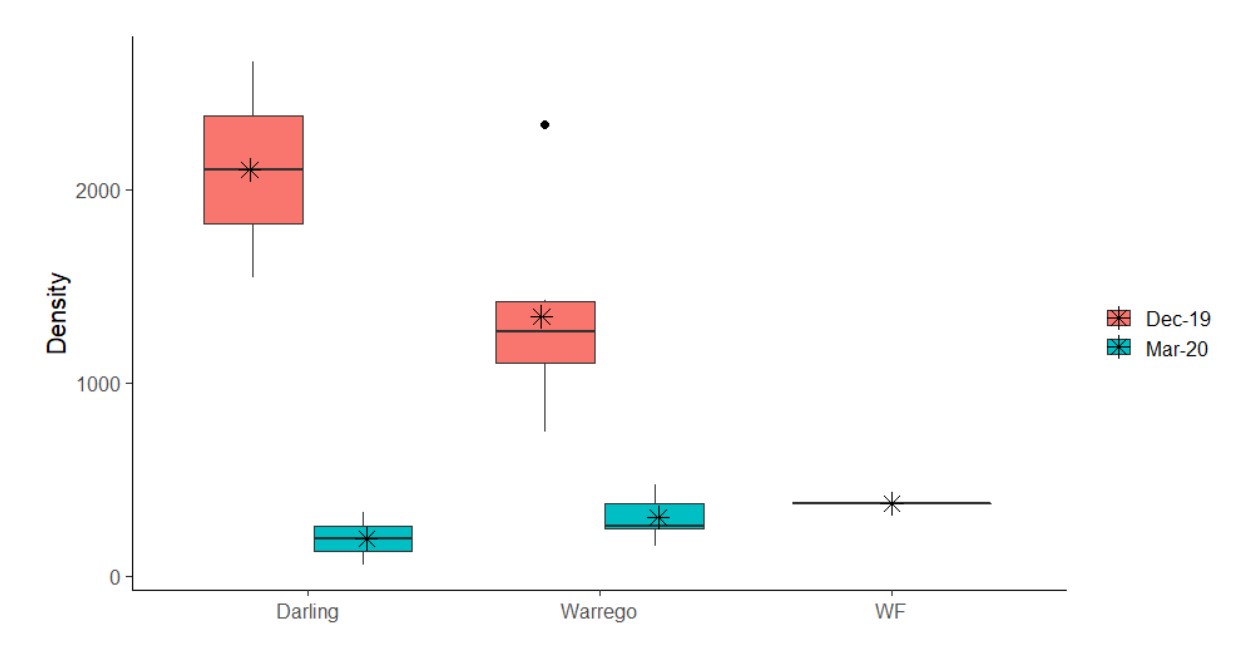


Figure 7 Ranges in microinvertebrate density (individuals/L) from the Pre- (Dec 2019) and During (Mar 2020) flows in the 2019-2020 water year across the three zones. Horizontal black lines indicate medians and asterisks means.

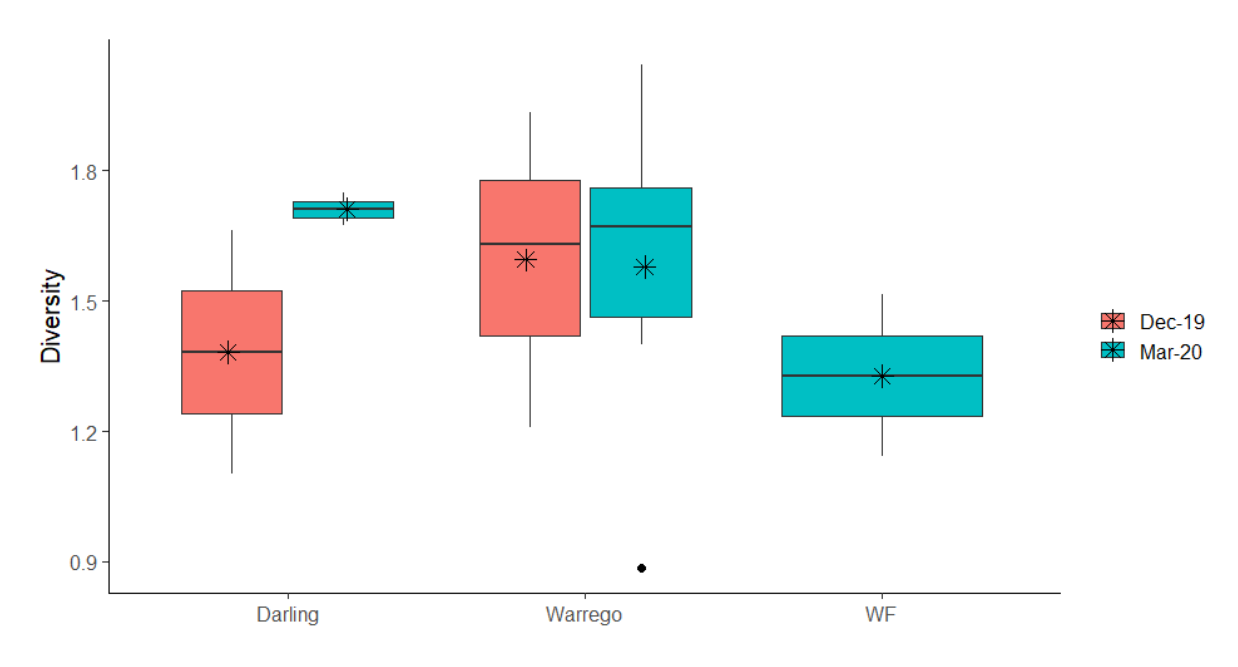


Figure 8 Ranges in Shannon Weiner Diversity of microinvertebrate communities from the Pre- (Dec 2019) and During (Mar 2020) flows in the 2019-2020 water year across the three zones. Horizontal black lines indicate medians and asterisks means.

#### 3.1.4 Macroinvertebrates

Macroinvertebrate richness remained similar between Times and among Zones (Figure 9). Macroinvertebrate density did not differ between Times when analysed across all Zones ( $F_{1,14}$ =4.079, p=0.063). However, Warrego (0.3 ± 0.2 individuals/L, p<0.005) and the Western Floodplain (0.4 ± 0.2 individuals/L, p<0.005) had higher densities than the Darling (0.1 ± 0.1 individuals/L;  $F_{2,14}$ =10.861, p<0.001, Figure 10) but patterns within Zones were inconsistent across Time ( $F_{2,14}$ =4.722, p=0.027). Shannon diversity of macroinvertebrates remained similar among Zones and Times (Figure 11).

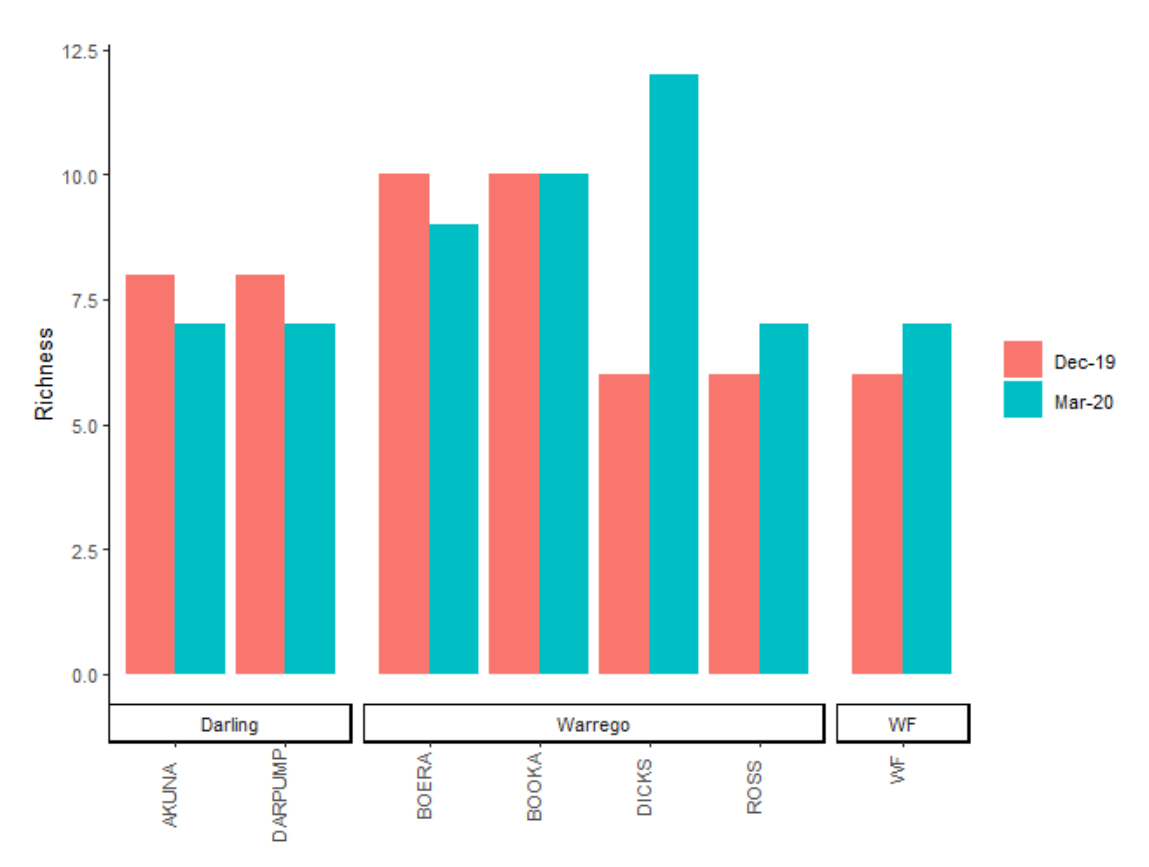


Figure 9 Macroinvertebrate richness Pre- (Dec 2019) and During (Mar 2020) Flow Event 1 in the 2019-2020 water year across Sites in the three Zones in the Selected Area.

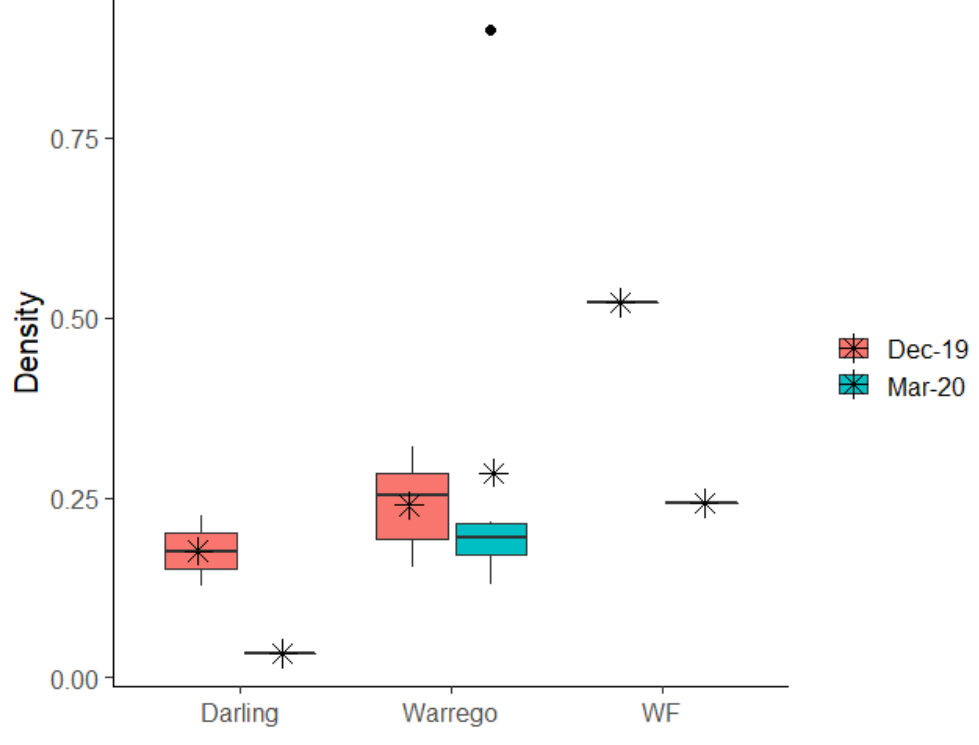


Figure 10 Ranges in macroinvertebrate density (individuals/L) from Pre (Dec 2019) and During (Mar 2020) the February-May 2020 flows in the 2019-2020 water year across the three Zones in the Selected Area. Horizontal black lines indicate medians and asterisks means.

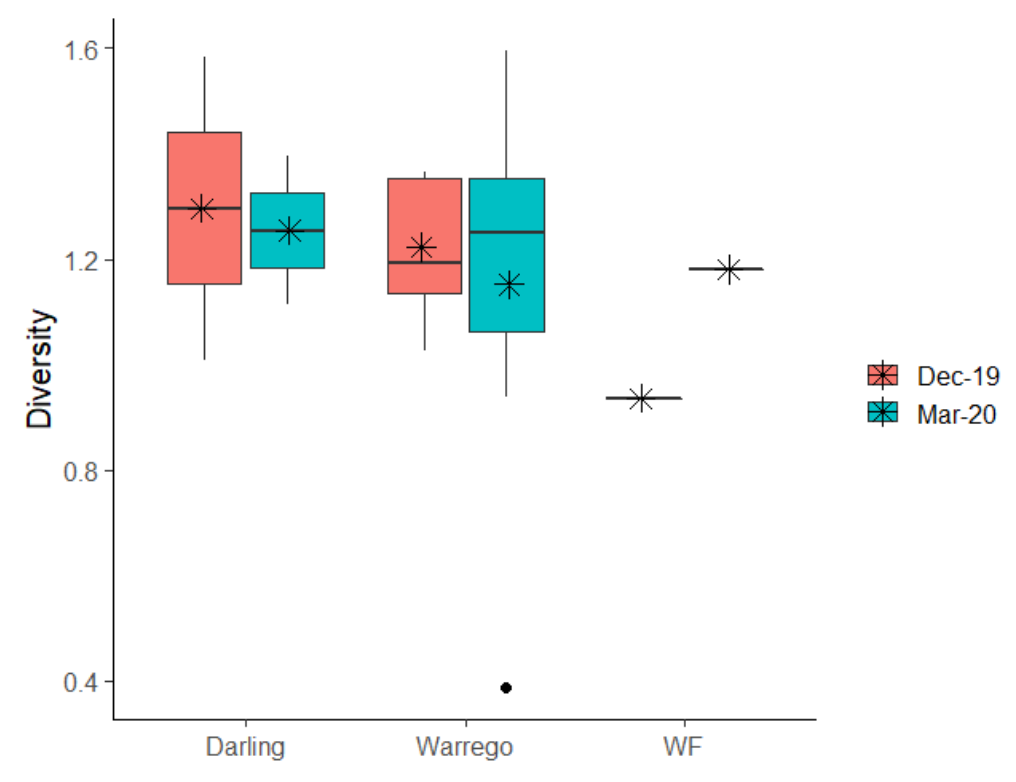


Figure 11 Ranges in Shannon Weiner Diversity of macroinvertebrate communities from the Pre- (Dec 2019) and During (Mar 2020) February-May 2020 in the 2019-2020 water year across the three Zones in the Selected Area. Horizontal black lines indicate medians and asterisks means.

# 3.1.5 Invertebrate community composition

Time explained the greatest difference in invertebrate community composition (61%), with density decreasing during the flow event (Figure 12), followed by Sites within Zones (8%, Table 6). Analysis of presence/absence data showed that the community changed from one dominated by benthic microcrustaceans (harpacticoids and ostracods) to one dominated by pelagic microcrustaceans (Bosminidae and Daphniidae) and free-living nematodes following inundation (Figure 13). The invertebrate community in the Darling sites differed in taxa to both the invertebrate communities in the Warrego and Western Floodplain, with the latter two supporting similar assemblages (Figure 13, pseudo F=3.5, p<0.01; explains 18% of community variation).

Changes to invertebrate community composition between sampling Times correlated most strongly with water temperature (Pearson's r=-0.648; along the x-axis of Figure 14), with densities decreasing as water temperature decreased. The second strongest correlation was the separation in community composition along the y-axis due to GPP (Pearson's r=-0.452, Figure 14, Table 7).

Table 6 PERMANOVA results for invertebrate communities. (p/a) is presence/absence, ns is non-significant test result. The percentage of variation explained by each significant source of variation is given in brackets after the pseudo F value. \*\* represents p < 0.01 and \*\*\* represents p < 0.001.

Source of variation	Assemblage (density)	Assemblage (p/a)	Richness	Diversity
Time	21.1*** (61%)	8.7*** (36%)	ns	ns
Zone	ns	3.5** (18%)	ns	ns
Site (Zone)	1.8* (8%)	ns	ns	ns
Time x Zone	ns	ns	ns	ns

Table 7 Pearson's r values for correlations with community composition and productivity parameters. MDS1 is the x-axis and MDS2 is the y-axis of Figure 13, respectively.

	Mean GPP	Mean ER	Mean NPP	Mean P:R	Water temperature (°C)
MDS1	-0.293	-0.188	0.156	-0.012	-0.648
MDS2	-0.453	-0.295	0.248	0.092	-0.207

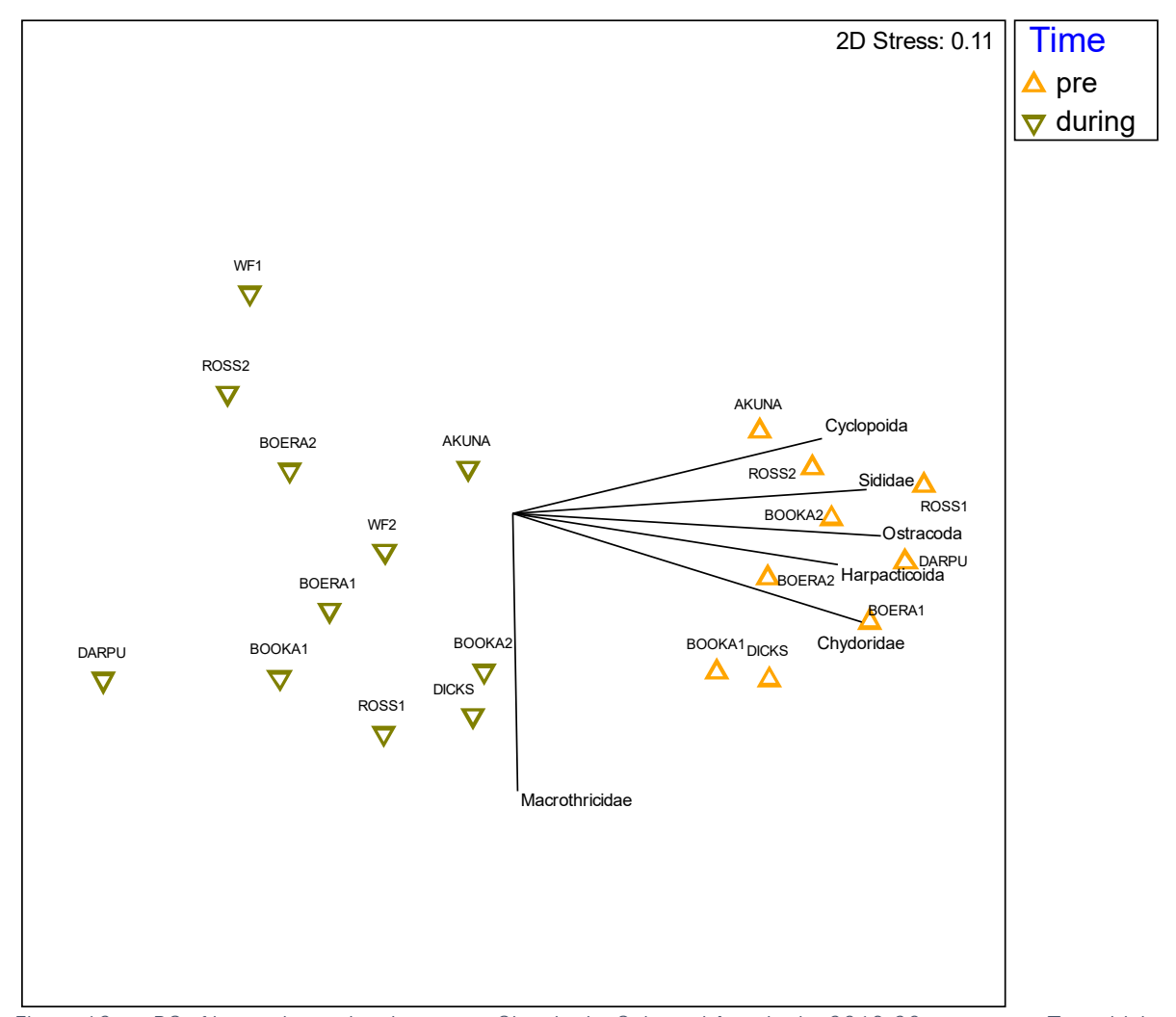


Figure 12 nmDS of invertebrate density among Sites in the Selected Area in the 2019-20 water year. Taxa driving differences are shown as vectors with density decreasing from right to left.

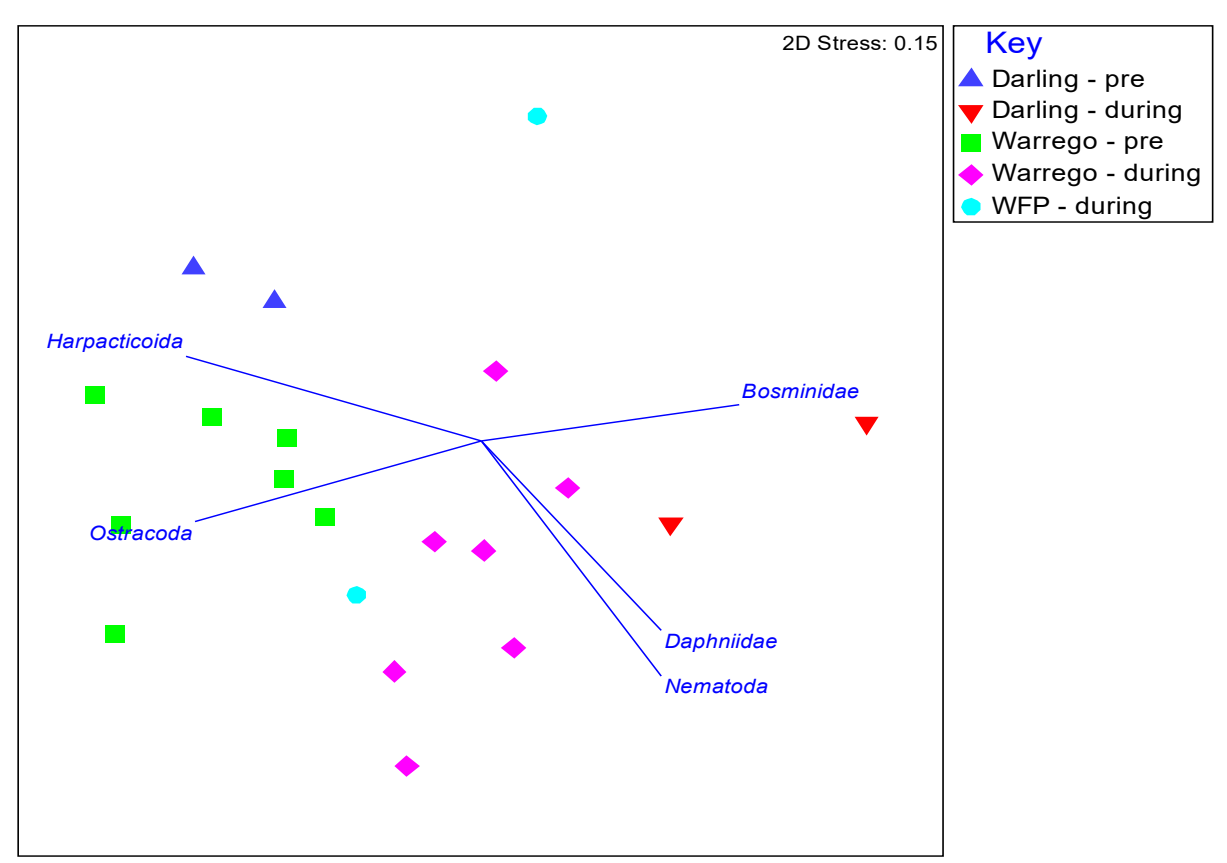


Figure 13 nMDS of invertebrate presence/absence among Sites in the Selected Area in the 2019-20 water year. Taxa driving differences are shown as vectors.

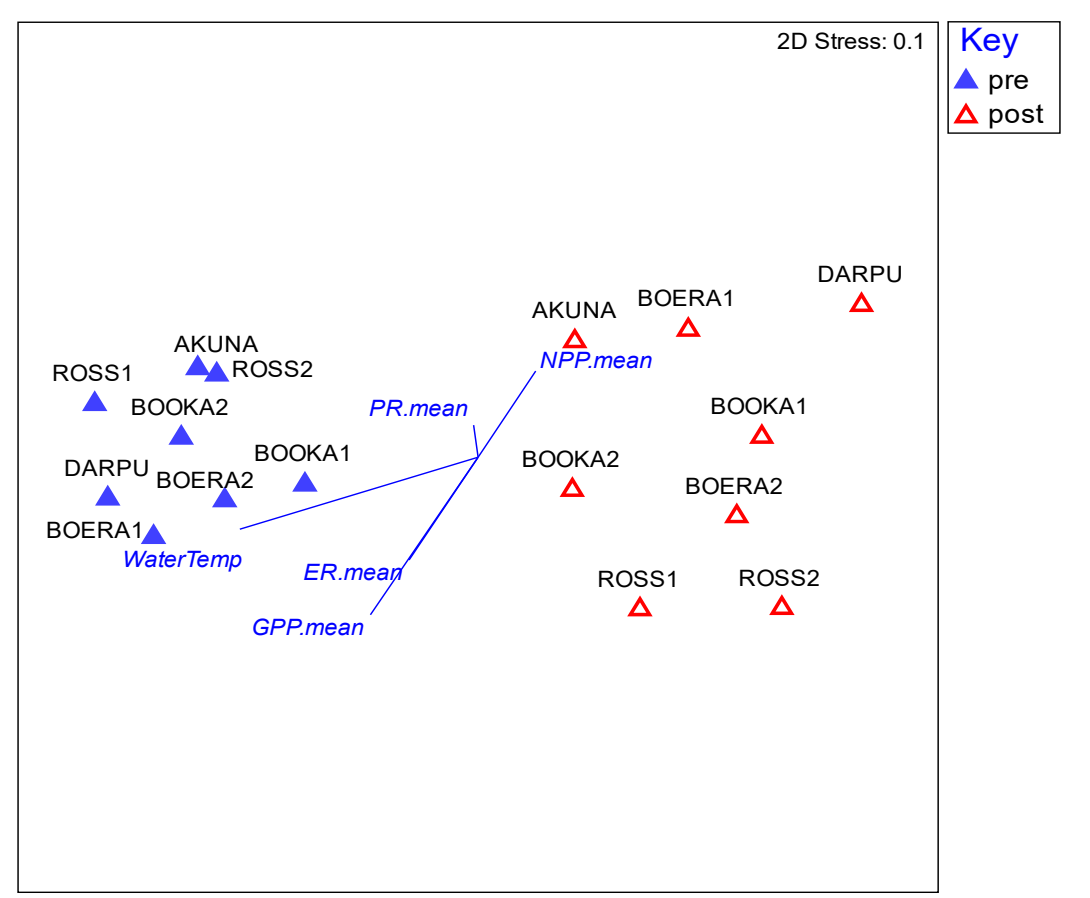


Figure 14 nMDS of invertebrate densities among Sites in the Selected Area in the 2019-20 water year. Water temperature, GPP, ER and NPP are shown as vectors.

## 3.2 Multi-year comparisons

#### 3.2.1 Metabolism

Given the change in monitoring approach, and limited data availability due to failure of the YSI Hydrolab water quality multiprobes at DARPUMP and AKUNA and the limited acceptance of BASE model outputs, only limited additional 2019-20 data points in the Darling River were added. Thus, further analyses of metabolism will be conducted in the 2020-21 water year to extend the detailed water quality and stream metabolism findings given in the 2018-19 annual report.

#### 3.2.2 Microinvertebrates

There were no consistent patterns in microinvertebrate richness among Zones over the 6 years of the LTIM/MER project (Figure 15). However, annual differences were significant ( $X^2_{3,82}$ =6.862, p<0.001), and these were driven by lower average microinvertebrate richness in 2016-17 (8.3 ± 2.1) than 2015-16 (10.8 ± 1.4; p<0.001) and 2017-18 (10.1 ± 2.0, p<0.01). While average microinvertebrate richness was lowest across all zones in 2016-17, it was also extremely variable within zones (Figure 15).

Density was also highly variable in 2016-17, particularly within the Warrego and Western Floodplain sites (Figure 16). However, in contrast to richness, microinvertebrate mean densities peaked in 2016-17 (14,374  $\pm$  20,739 individuals/L, Figure 16,  $F_{3,77}=35.959$ , p<0.001), and have been much lower during the drier 2017-18 (2,553  $\pm$  1,628 individuals/L, p<0.001) and 2019-20 (834  $\pm$  742 individuals/L, p<0.001) water years. The decrease in microinvertebrate densities from 2017-18 to 2019-20 was significant (p<0.001). The Western Floodplains supported the greatest microinvertebrate densities when inundated (13,815  $\pm$  23,461 individuals/L), followed by the Warrego (7,602  $\pm$  13,790 individuals/L), both of which were significantly greater (F<sub>2,77</sub>=4.971, p<0.01) than the Darling (2,547  $\pm$  2,191 individuals/L, p<0.05 and p<0.05, respectively). Shannon diversity of microinvertebrate communities followed similar patterns to richness, where diversity in 2016-17 (1.0  $\pm$  0.5) was significantly lower than in 2015-16 (1.4  $\pm$  0.4; p<0.01), 2017-18 (1.6  $\pm$  0.3; p<001) and 2019-20 (1.6  $\pm$  0.3; p<0.001, Figure 17).

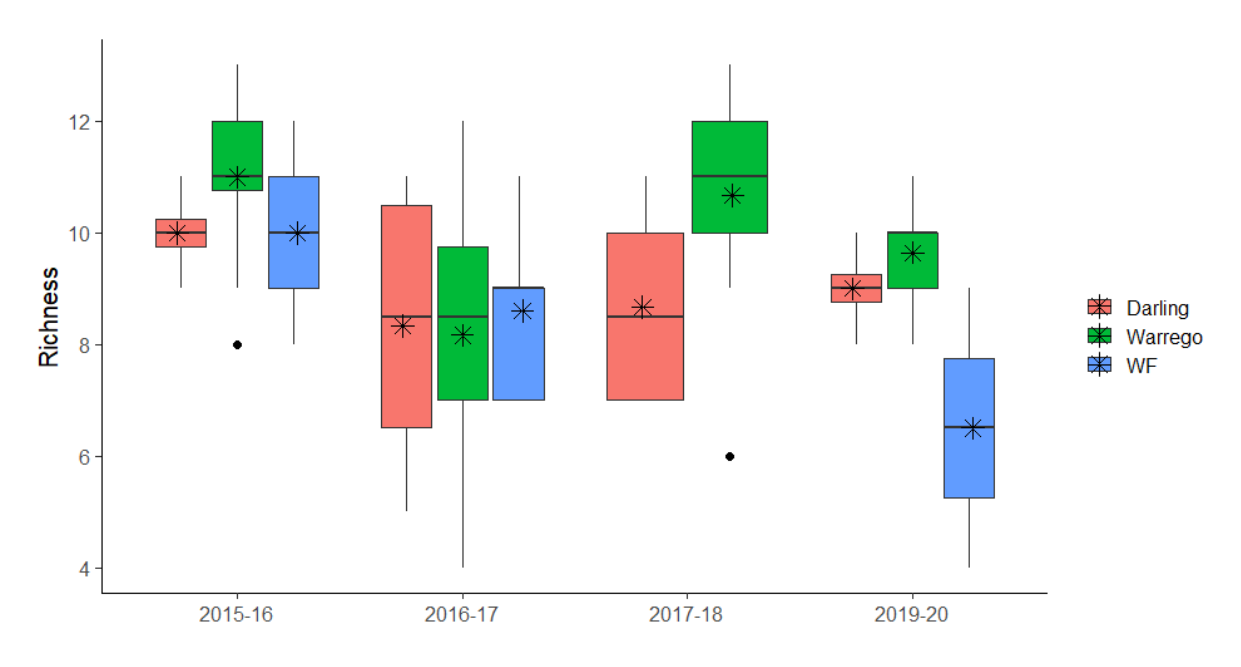


Figure 15 Ranges in macroinvertebrate richness over water years across the three Zones in the Selected Area. Horizontal black lines indicate medians and asterisks means.

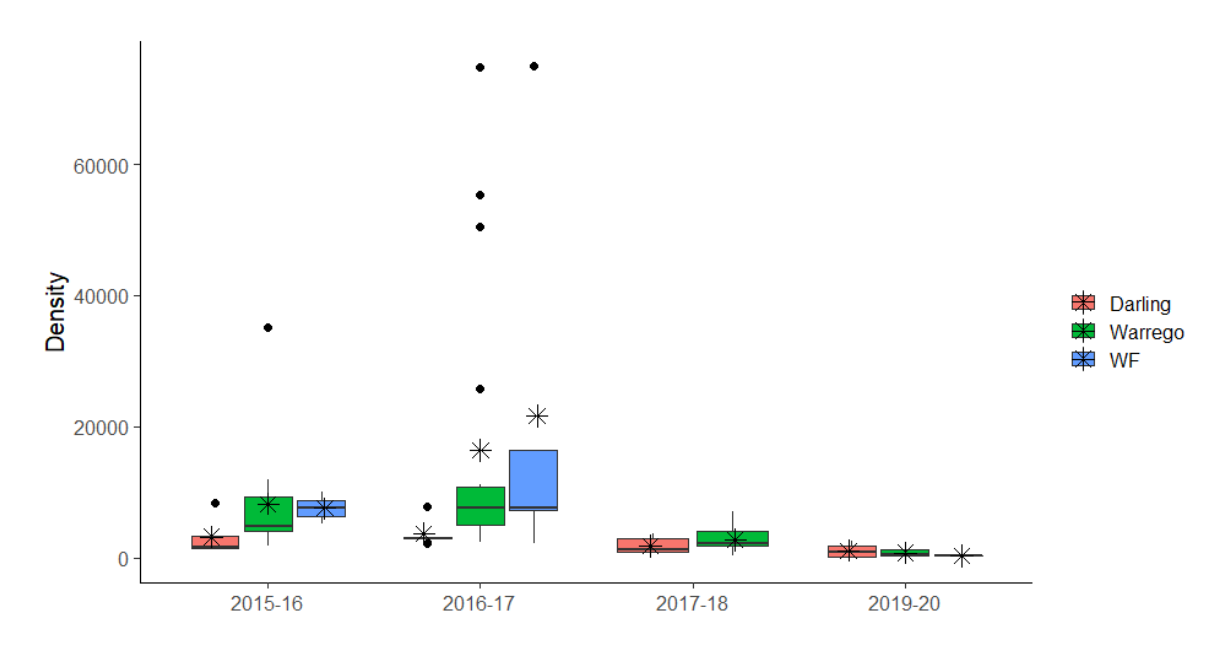


Figure 16 Ranges in macroinvertebrate density (individuals/L) over water years across the three Zones in the Selected Area. Horizontal black lines indicate medians and asterisks means.

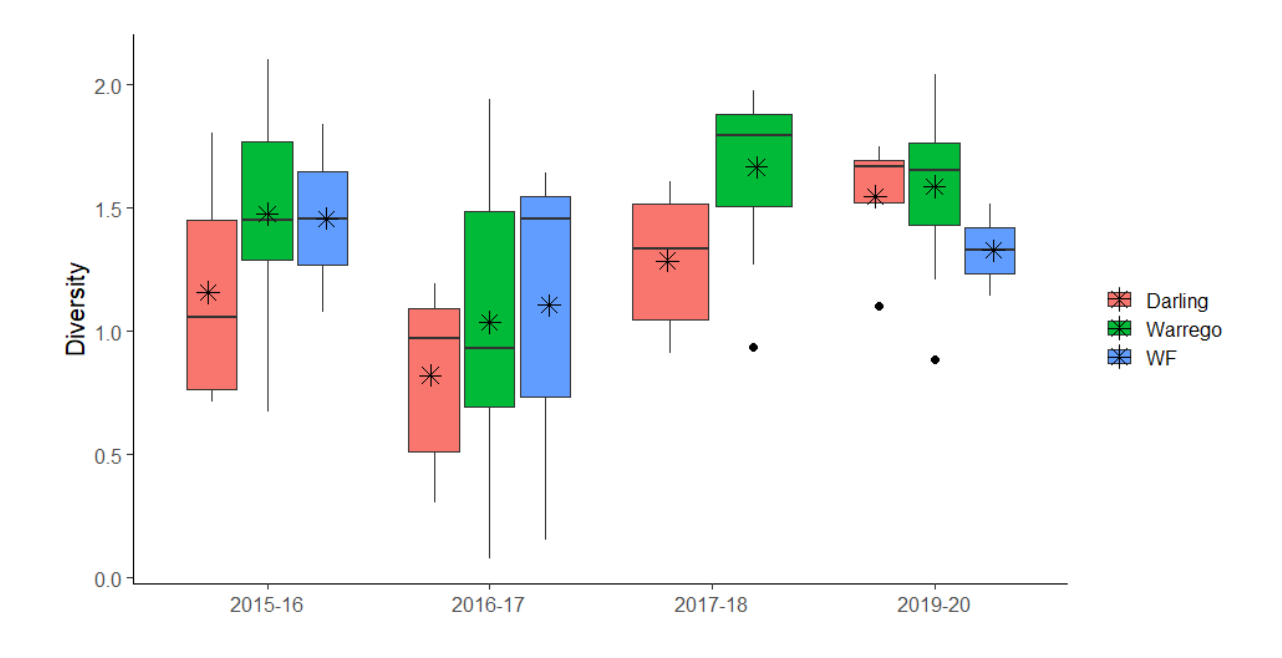


Figure 17 Ranges in macroinvertebrate Shannon diversity over water years across the three Zones in the Selected Area. Horizontal black lines indicate medians and asterisks means.

#### 3.2.3 Macroinvertebrates

Macroinvertebrate richness averaged 8  $\pm$  3 taxa from 2015 to 2020 (Figure 18), but there were no significant differences among Zones ( $X^2_{2,85}$ =1.164) or Years ( $X^2_{3,82}$ =0.965). When inundated, Western Floodplain macroinvertebrate communities have higher densities (0.5  $\pm$  0.3 individuals/L) than the Warrego waterholes (0.3  $\pm$  0.0 individuals/L, p<0.05) or the Darling River (0.1  $\pm$  0.1 individuals/L, p<0.001), and the Warrego waterholes have higher densities than the Darling River (p<0.001, Figure 19). This pattern of Western Floodplain > Warrego > Darling was consistent over Time. In contrast, there were no significant differences amongst Shannon diversity over Time or Zones (Figure 20).

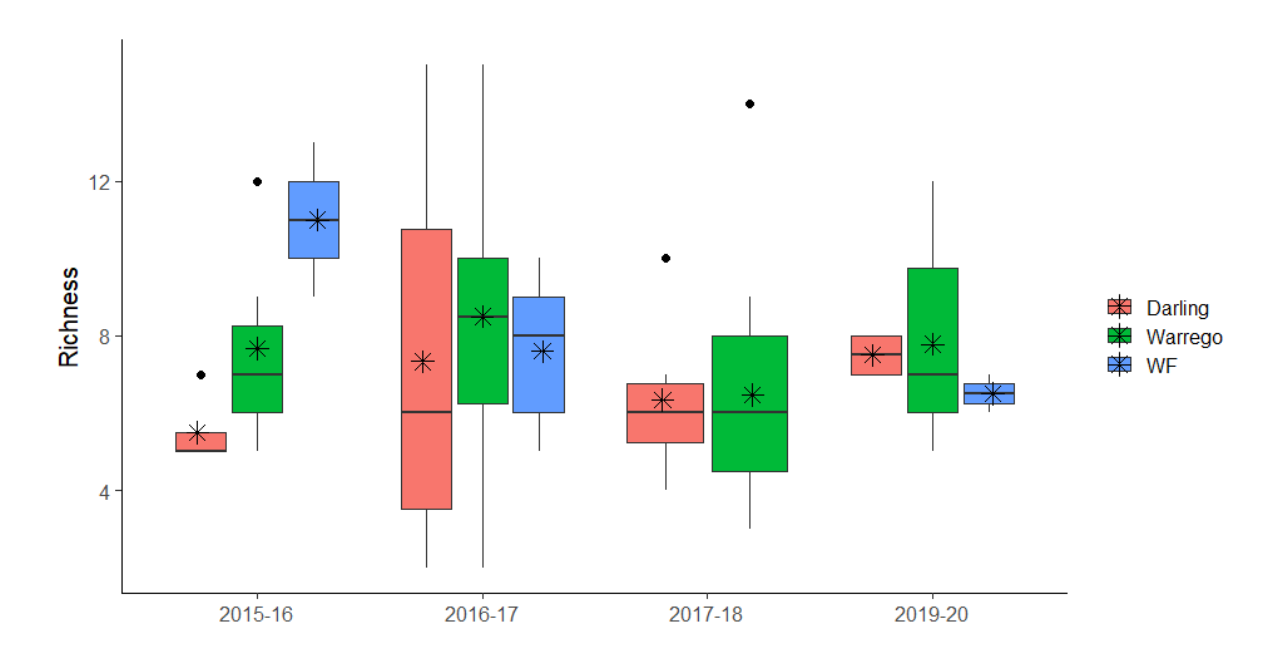


Figure 18 Macroinvertebrate richness across Zones in the Selected Area through the 2015-16 to 2019-20 water years. Black horizontal lines represent medians, asterisks means and dots outlying samples.

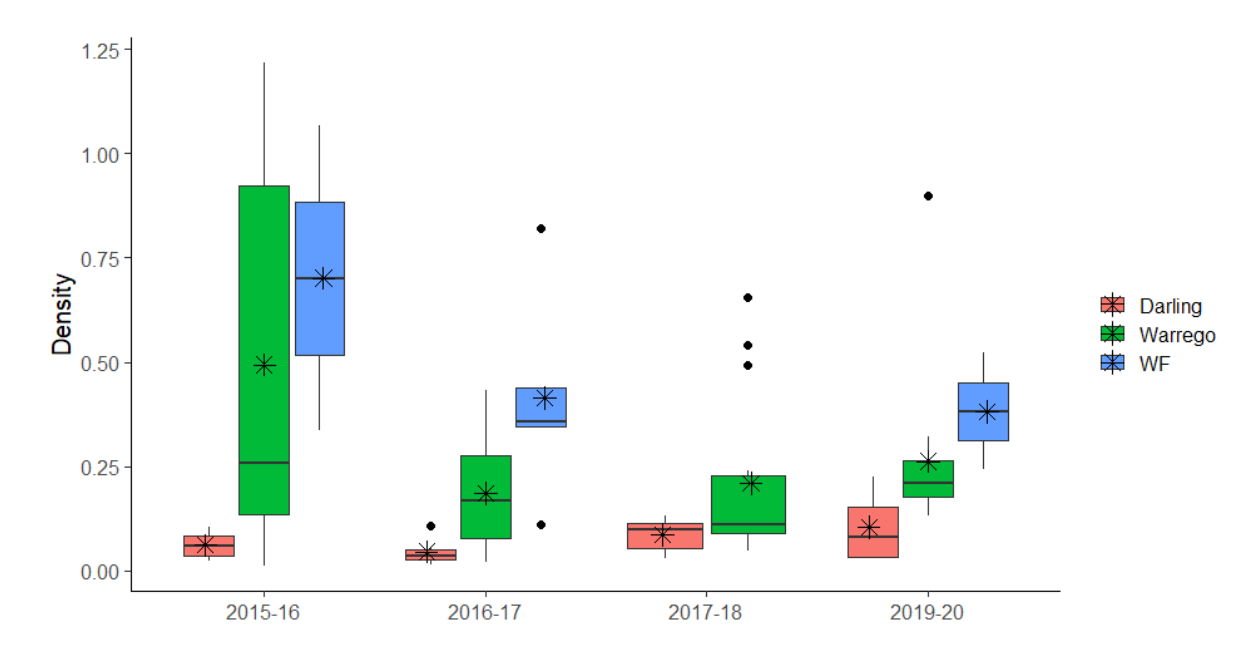


Figure 19 Macroinvertebrate density (individuals/L) across Zones in the Selected Area through the 2015-16 to 2019-20 water years. Black horizontal lines represent medians, asterisks means and dots outlying samples.

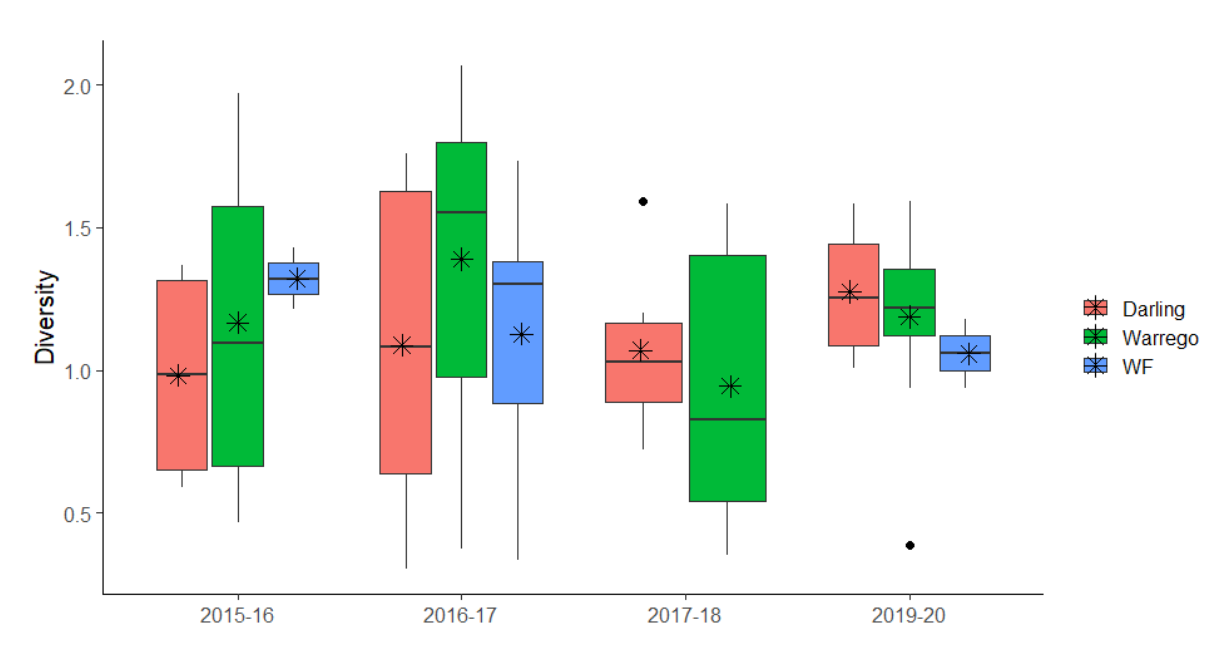


Figure 20 Macroinvertebrate Shannon diversity across Zones in the Selected Area through the 2015-16 to 2019-20 water years. Black horizontal lines represent medians, asterisks means and dots outlying samples.

# 4 Discussion and conclusion

Monitoring was undertaken pre, during and post a large flow event that occurred from late February-May 2020 for water quality, metabolism and microinvertebrates and macroinvertebrates in the Darling River and Warrego River channels and the Western Floodplain with the aim of understanding the connections among flow, inundation, and primary and secondary productivity. The limited water quality and nutrient data recorded for the channel and floodplain sites due to COVID-19 travel restrictions on field work were unable to identify if water for the environment improved water quality during this event. However, conductivity and pH remained within ANZECC guidelines throughout the Selected Area, including before the event when the region was in severe drought. Turbidity significantly decreased in the Darling River during the event and previous monitoring indicates that this contributed to higher GPP. Aligned with high turbidity, TN and TP concentrations significantly exceeded ANZECC guidelines at all sites over the 2019-20 water year. NOx concentrations were greatest in the Darling River and increased in both the Darling and Warrego Rivers during the watering event. In contrast, concentrations in the Western Floodplain were comparatively low and decreased during the inundation. This was likely due to rapid uptake and cycling during an algal bloom that fuelled significant invertebrate production on the Western Floodplain.

Despite consistently high nutrient concentrations at all sites that should drive primary productivity, rates of stream metabolism continued to be highly variable and strongly heterotrophic, regulated by very high turbidity and poor light availability at all sites and times. Both the Darling and Warrego Rivers were carbon sinks, consuming significantly more carbon than they produced, although the Warrego had lower rates than the Darling. ER and NPP both peaked in mid-February during the flow event when water

temperatures remained high, consistent with the long-term pattern showing that temperature is a major regulator of primary production in these systems.

Acceptance rates of data output from the BASEv2 model continues to be very low and hinders the ability to examine long-term trends in rates of metabolism. This was the first year in which productivity was measured in the Warrego River and the data had greater acceptance rates by the BASEv2 model than those recorded in the Darling River, ranging from 7.6% to a maximum of 16.6% acceptance of model outputs. The underwater light climate, high temperatures and very low rates of oxygen production continue to confound the BASE model used to determine rates of production.

The microinvertebrate communities were distinct among the Warrego, Darling and Western Floodplain zones. Richness did not increase with increased inundation, likely because communities were already well developed by summer 2019. The Western Floodplain supported fewer taxa during its initial inundation phase compared with the more hydrologically stable Darling and Warrego zones. Density declined as incoming discharge diluted existing and emergent invertebrate populations. Consistent with longterm observations, when inundated, the Western Floodplain supports greater microinvertebrate densities than the Warrego River, which is significantly greater than densities in the Darling River. However, overall microinvertebrate densities were lower than the peak observation during 2016-17 high flow event. In contrast, macroinvertebrate communities were taxonomically similar across the zones, with density following previously observed patterns of the Western Floodplain supporting the highest densities when inundated, followed by the Warrego then Darling Rivers. The 2019-20 water year produced the lowest mean richness, density and diversity compared with other inundation events on the Western Floodplain. The magnitude of the event in connecting the floodplain to the Darling River for the first time in over a decade highlights the volume of water on the floodplain, suggesting the dilution effect on density and richness apparent in the channel habitats may also apply to floodplain habitats. Our inability to include post event microinvertebrate and macroinvertebrate data also prevents us from reporting on the influence of the inundation and contraction cycle on food webs at this point in time, but will be incorporated into the 2020-21 annual report.

The invertebrate community was dominated by benthic microcrustaceans such as harpacticoids and ostracods before the 2020 flow event. This shifted to a dominance of pelagic microcrustaceans such as Bosminidae and Daphniidae during the event, taxa that are known to be an important food suppy for juvenile fish recruits. Increased GPP during the same period suggests an increase in primary productivity within the water column and aligns with the increase in taxa such as Daphniidae that are algal grazers. The contribution of benthic free-living nematodes also significantly increased during the event; these are predominantly detritivores that break down organic matter and play a key role in decomposition and nutrient remineralisation, and therefore contribute to increased rates of ER. The Darling supported low densities of microinvertebrates and macroinvertebrates compared with the Warrego despite the greater production of carbon (food supply) in the Darling. This suggests that reduced habitat complexity or availability in the Darling rather than food availability may be limiting secondary productivity.

The establishment of metabolism monitoring stations along the Warrego improves the survey design and improves the link between water quality and nutrient conditions with invertebrate production within the Selected Area. Additional work during the 2020-21 water year to increase the proportion of metabolism data accepted to the BASE model, will continue to improve our understanding of how water for the environment drives metabolism and food webs in the Selected Area.

### 5 References

ANZECC (Australian – New Zealand Environment and Conservation Council) (2000). Australian and New Zealand Guidelines for Fresh and Marine Water Quality, vol 1, The Guidelines, pp 314.

Clarke, K. R. W., Warwick, R. M. 2001. Change in Marine Communities: An Approach to Statistical Analysis and Interpretation. 2nd edition. *PRIMER-E*.

Grace, M. R., Giling, D. P., Hladyz, S., Caron, V., Thompson, R. M., & Mac Nally, R. 2015. Fast processing of diel oxygen curves: Estimating stream metabolism with BASE (BAyesian Single-station Estimation). *Limnology and Oceanography: Methods, 13*(3), 103-114.

Hale J., Stoffels R., Butcher R., Shackleton M., Brooks S. & Gawne B. 2013. *Commonwealth Environmental Water Office Long Term Intervention Monitoring Project – Standard Methods.* Final Report prepared for the Commonwealth Environmental Water Office by The Murray-Darling Freshwater Research Centre, MDFRC Publication 29.2/2014, January, 182 pp.

Masaaki Hosomi & Ryuichi Sudo (1986) Simultaneous determination of total nitrogen and total phosphorus in freshwater samples using persulfate digestion, International Journal of Environmental Studies, 27:3-4, 267-275, DOI: 10.1080/00207238608710296.

Murphy, J. and Riley, J.P. (1958). A single-solution method for the determination of soluble phosphate in sea water. Journal of the Marine Biological Association of the UK, 37: 9-14.